MENU 2007
11th International Conference
on Meson-Nucleon Physics and
the Structure of the Nucleon
September10-14, 2007
IKP, Forschungzentrum Jülich, Germany

BARYON SPECTROSCOPY WITH INELASTIC CHANNELS

A. Starostin[1] *and S. Prakhov*
Department of Physics and Astronomy
University of California, Los Angeles
Los Angeles, CA 90095-1547, USA

Abstract

Many properties of QCD in the non–perturbative regime remain unknown. Baryon spectroscopy plays a vital role in understanding the confinement mechanism and origin of mass. Two series of successful experiments in the area of baryon spectroscopy have been conducted with the Crystal Ball detector with the pion and kaon beams of Brookhaven AGS. New high accuracy total and differential cross sections as well as hyperon polarizations are presented for the reactions $K^-p \to \pi^0\Sigma$, $K^-p \to \pi^0\Lambda$, and $K^-p \to \overline{K}^0 n$. The Crystal Ball program continues at the upgraded Mainz Microtron, which provides a high intensity beam of linearly and circularly polarized real photons up to the maximum energy of 1.5 GeV. Some preliminary MAMI-C results are shown.

1 Introduction

While QCD gives a good description of the strong interactions at short distances in the asymptotic region [1], processes in the non–perturbative regime cannot be analytically calculated due to the strong increase of the running coupling constant at large distances. For example, it is still insufficiently understood how the asymptotically observed hadrons, including their rich resonance spectrum, are created from QCD dynamics [2]. This is one of the reasons why one makes use of phenomenological, QCD-inspired, approaches to the description of hadron interaction at low and intermediate energies. The accurate experimental determination of the resonance parameters is a vital factor in our understanding of the nature of hadrons. Among the least studied is the hyperon sector [3]. Kaon beams are not readily available and there are experimental difficulties in detecting the complex decays of the Λ^*

[1]E–mail:starost@ucla.edu

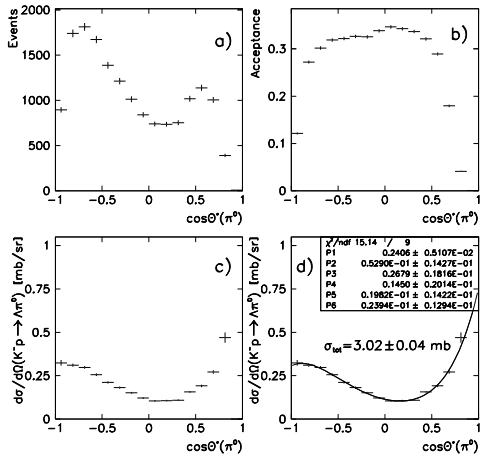

Figure 1: Angular distributions of the Λ in the center-of-mass for the reaction $K^-p \to \pi^0\Lambda$ at a beam momentum of 714 MeV/c. (a) event distribution as measured, (b) acceptance, (c) differential cross section, (d) Legendre polynomial fit to our data and the resulting total cross section.

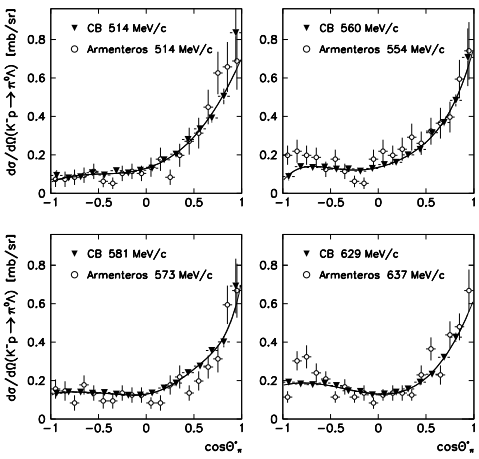

Figure 2: The CB differential cross sections for $K^-p \to \pi^0\Lambda$ compared to the results by Armenteros [5].

and Σ^*. Most of the existing hyperon data come from old bubble chamber experiments (see Refs [4, 5], for example) and suffer from statistical limitations.

The last experiment studying exited Λ^* and Σ^* was conducted at Brookhaven National Laboratory (BNL). The experiment utilized the Crystal Ball multiphoton spectrometer installed at a secondary beam line of the Alternative Gradient Synchrotron (AGS). The details of the experimental setup as well as the analysis technique are described in Refs. [6–9]. Here we present new results on the total and the differential cross sections for $K^-p \to \pi^0\Sigma$, $K^-p \to \pi^0\Lambda$, and $K^-p \to \overline{K}^0 n$. We have also measured the polarization of the hyperon in the reactions $K^-p \to \pi^0\Sigma$, $K^-p \to \pi^0\Lambda$.

2 Kaon induced reactions

The candidates for reactions $K^-p \to \pi^0\Lambda$ and $K^-p \to \overline{K}^0 n$ were selected from the four– and five–cluster events. For the four–cluster events it was assumed that all clusters originate from photons and the neutron is the missing particle. The five–cluster events were analyzed as if the neutron was detected in the Ball. The events were fitted to the hypotheses $K^-p \to K^0_S n \to 2\pi^0 n \to 4\gamma n$ and $K^-p \to \pi^0\Lambda \to 2\pi^0 n \to 4\gamma n$ for all possible permutations of four photons, or four photons and a neutron. The z coordinate of the interaction vertex and the decay length of the Λ and the K^0_S were the free parameters of the fit. The combination with the largest confidence level (CL) was used to reconstruct the kinematics of the reactions assuming that the CL is larger than 5%. In some cases an event satisfies both hypothesis. Such event was used only if the CL for one of the reaction exceeded the CL for the another reaction by a factor of two. This procedure allowed to decrease the background from misidentification to less than 4%, while retaining the optimum number of good event candidates. Figure 1 shows the intermediate steps and the final differential cross section for the $K^-p \to \pi^0\Lambda$ at the kaon beam momenta of 714 MeV/c. For the cross section calculations we used the PDG branching ratio of $BR(\Lambda \to \pi^0 n) = 0.358 \pm 0.005$ and $BR(K^0_S \to \pi^0\pi^0) = 0.3139 \pm 0.0028$ [10]. The examples of the resulting differential cross sections for the reactions $K^-p \to \pi^0\Lambda$ and $K^-p \to \overline{K}^0 n$ are shown in Figs. 2 and 3. The systematical uncertainty of about 7% comes from the uncertainty in the number of kaons in the beam and from the uncertainty in the fraction of good events lost due to pile-up in the CB. The systematical uncertainty is not shown on Figs 2, 3, and 5. The details of the data analysis are given in Ref. [11]. The polarization of the Λ was measured via its decay asymmetry as described in Ref. [5]. Examples of our results for the Λ polarization multiplied by the differential cross section of $K^-p \to \pi^0\Lambda$ are shown in Fig. 4 in comparison with the results from Ref. [5].

The candidates for the reaction $K^-p \to \pi^0\Sigma$ were selected from five–cluster (photons only) and six–cluster (photons and the neutron) events. All possible permutations were examined with the $K^-p \to \pi^0\Sigma^0 \to \pi^0\gamma\Lambda \to 2\pi^0\gamma n \to 5\gamma n$ hypothesis. The events with at least one combination satisfying the hypothesis at 5% CL were accepted. Some examples of the $K^-p \to \pi^0\Sigma$ differential cross sections and the Σ polarization are shown on Figs. 5 and 6.

While demonstrating superior quality the Crystal Ball data agrees with the existing data for the reactions $K^-p \to \pi^0\Lambda$ and $K^-p \to \overline{K}^0 n$. The discrepancy between the CB and the existing data for the differential cross

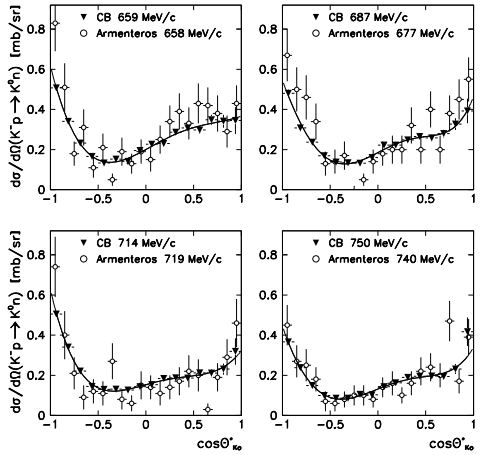

Figure 3: The CB differential cross sections for $K^-p \to \overline{K}^0 n$ compared to the results by Armenteros [5].

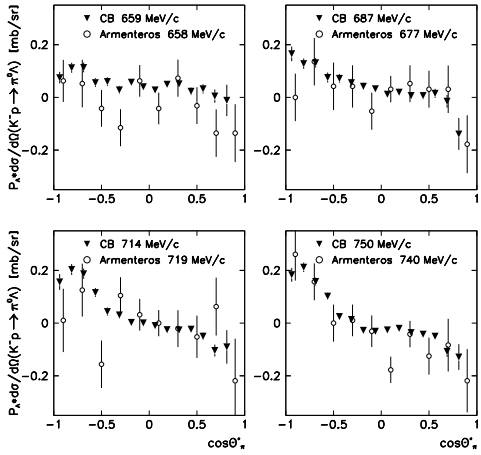

Figure 4: The product of the Λ polarization and the differential cross section for $K^-p \to \pi^0\Lambda$. The CB results are compared to the ones from Ref. [5].

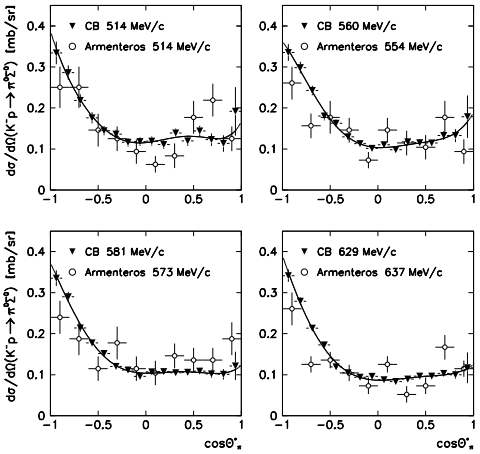

Figure 5: The CB differential cross sections for $K^-p \to \pi^0\Sigma^0$ compared to the results by Armenteros [5].

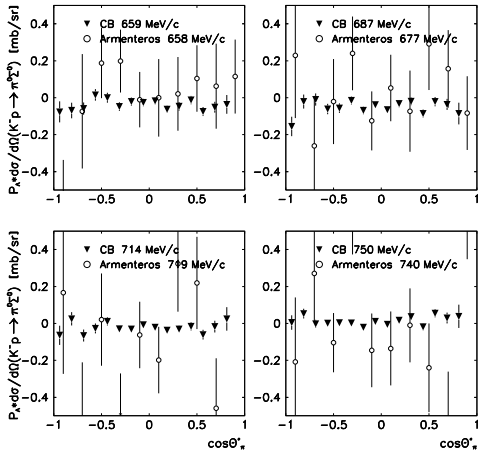

Figure 6: The product of the Σ^0 polarization and the differential cross section for $K^-p \to \pi^0\Sigma^0$. The CB results are compared to the ones from Ref. [5].

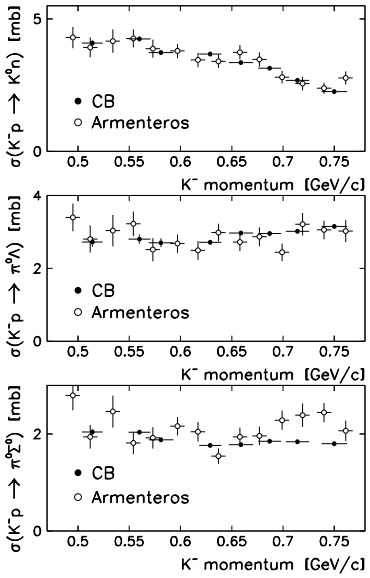

Figure 7: The CB results for the total cross section of reactions $K^-p \to \overline{K}^0 n$, $K^-p \to \pi^0\Lambda$ and $K^-p \to \pi^0\Sigma^0$ at different beam momenta compared to Armenteros [5].

sections $K^-p \to \pi^0\Sigma^0$ can be due to the difficulties in detecting a Σ^0 directly in a bubble chamber. It can lead to undersubtraction of the $\pi^0\Lambda$ and especially the $\pi^0\pi^0\Lambda$ backgrounds. A similar discrepancy is observed in the total cross sections of the reaction $K^-p \to \pi^0\Sigma^0$ for the different beam momenta with the corresponding results by Armenteros [5]. This comparison is given in Fig. 7 for all three reactions. The agreement between the total cross sections of the CB and of Armenteros [5] for the two other reactions is good. The measured total cross section do not indicate any significant structures from particular resonances. The resonances in this energy region are $\Lambda(1600)\frac{1}{2}^+$, $\Lambda(1670)\frac{1}{2}^-$, $\Lambda(1690)\frac{3}{2}^-$, $\Sigma(1580)\frac{3}{2}^-$, $\Sigma(1620)\frac{1}{2}^-$, $\Sigma(1660)\frac{1}{2}^+$, and $\Sigma(1670)\frac{3}{2}^-$. A more sophisticated partial–wave analysis is needed in order to extract the resonance parameters from the data.

3 Photoproduction of light mesons

A new experimental program studying light–meson photoproduction is under way at the Mainz Microtron Facility. Recently the MAMI microtron was upgraded to 1.508 GeV giving access to $\sqrt{s}$ up to 1.93 GeV. The scope of the physics topics is broad and includes: (i) measurement of the in–medium ω mass; (ii) tests of Chiral Perturbation Theory and C and CP invariance in η decays; (iii) tests of Chiral Perturbation Theory and C invariance in η'

decays; (iv) study of the reaction $\gamma p \to \eta\gamma' p$ and the magnetic moment of the $S_{11}^{+}(1535)$ resonance; (v) measurement of the polarization of the recoil nucleon in photoproduction; (vi) measurement of the photon asymmetry of the $^{16}O(\vec{\gamma}, pp)$ reaction for photons energies up to 400 MeV; (vii) determination of the helicity dependence of meson photoproduction off the proton; (viii) measurement of the G asymmetry in $\vec{\gamma}p \to p\pi^0$ and $\vec{\gamma}p \to n\pi^+$; (ix) determination of the helicity dependence of single and double pion photoproduction processes and the GDH integral on the neutron; (x) photoproduction of the η–meson on the neutron including the angular distributions and the double polarization observable E; (xi) photoproduction of neutral pseudoscalar mesons on the neutron; (xii) measurement of the polarization observables in coherent π^0 photoproduction off deuterium; (xiii) $K^0\Sigma^+$ photoproduction.

The experimental setup includes the Crystal Ball detector with the TAPS spectrometer used as a forward wall. The central tracker located inside the Crystal Ball cavity consists of two layers of the cylindrical wire chamber surrounded by the particle identification detector (PID). The PID is a barrel made of 24 plastic strips. The beam photons are tagged in the upgraded Glasgow–Mainz tagger, which allows the determination of the beam photon energy with a typical accuracy of ± 2 MeV. A separate tagger ladder with fine segmentation called microscope can be used to improve the energy resolution to about ± 0.5 MeV.

The first MAMI-C run with real photons took place in March 2007. By October 2007 about 700 hours of data has been collected. One goal of the first months of running was to collect sufficient statistics for the experiments studying the decays of η and η'. Figure 8 shows the invariant mass of two photons in $\gamma p \to \gamma\gamma p$ obtained with the MAMI-C photon beam. The two peaks correspond to the $\pi^0 \to \gamma\gamma$ and $\eta \to \gamma\gamma$ decays. The resolution for the η peak is about 5%. Figure 9 shows the invariant mass of $\pi^0\gamma$; the peak is from $\omega \to \pi^0\gamma$ and the background under the peak is from the $\gamma p \to \pi^0\pi^0 p$ reaction.

One of the major goals of the first stage of the MAMI-C experiment is to collect the world largest samples of η and η'. The η sample will be used to calculate with high precision the slope parameter α of the $\eta \to 3\pi^0$ Dalitz plot [9] and the branching ratio and the matrix element of the $\eta \to \pi^0\gamma\gamma$ decay [6]. Both measurements will be used to test the Chiral Perturbation Theory predictions. The sample of η' events will allow an investigation of the $\eta' \to \eta\pi^0\pi^0$ and $\eta' \to 3\pi^0$ Dalitz plots [12]. Those distributions carry information on the $\pi\pi$ and $\eta\pi$ interactions and potentially can be used to measure the $\pi\pi$ scattering length [13].

The invariant mass of $\pi^0\pi^0\pi^0$ is shown on Fig. 10. The resolution of the peak is about 5 MeV after the fit to the $\gamma p \to 3\pi^0 p$ hypothesis. The

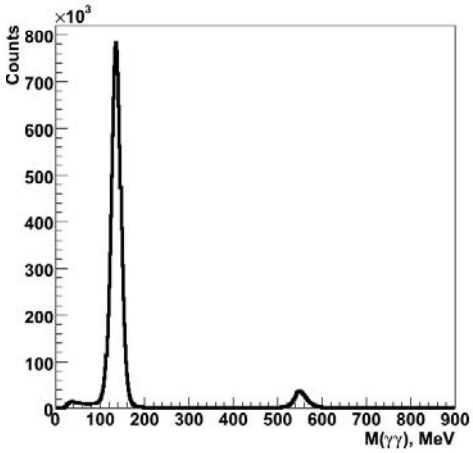

Figure 8: The invariant mass of two photons in $\gamma p \to \gamma\gamma p$ obtained with the MAMI-C photon beam. The two peaks correspond to the $\pi^0 \to \gamma\gamma$ and $\eta \to \gamma\gamma$ decays. The resolution for the η peak is about 5%.

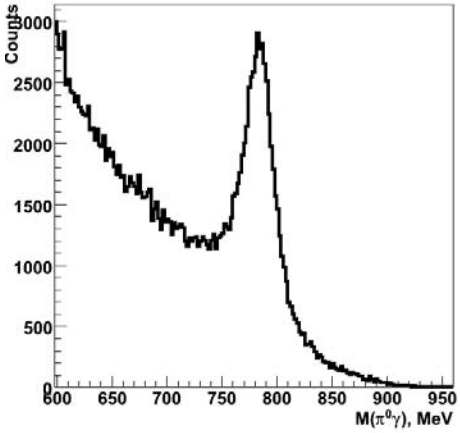

Figure 9: The invariant mass of $\pi^0\gamma$; the peak is from the $\omega \to \pi^0\gamma$ and the background under the peak is from $\pi^0\pi^0$ production.

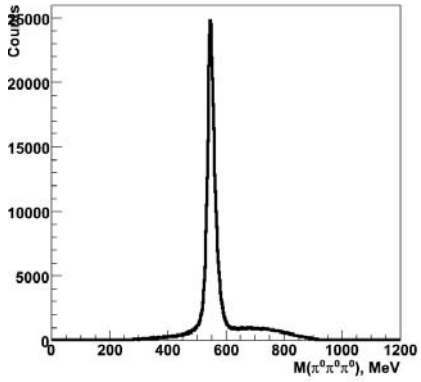

Figure 10: The invariant mass of $3\pi^0$ in $\gamma p \to 3\pi^0 p$ obtained at the MAMI-C. The peak is from the $\eta \to 3\pi^0$ decay. The resolution for the η peak is about 5 MeV after the fit. The background under the peak is from the direct production of $3\pi^0$'s.

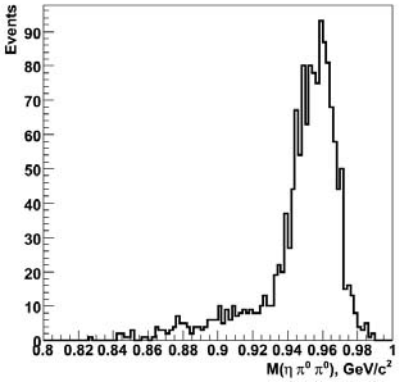

Figure 11: The invariant mass of $\eta\pi^0\pi^0$; the peak is from the $\eta' \to \eta\pi^0\pi^0$ decay.

background under the peak is from the direct production of the three π^0's via the cascade decay of the resonances. The experimental acceptance for the reaction is about 40% detecting all six photons and the proton. The total number of about 5×10^6 reconstructed $\eta \to 3\pi^0$ events is already collected in the experiment. Currently this is a world largest sample of such events.

The invariant mass of $\eta\pi^0\pi^0$ is shown on Fig. 11. The data shown here represent about 20% of the available statistics. The largest world sample of about 5000 events was collected by the GAMS2000 collaboration [12], therefore our sample is already comparable to the GAMS2000. The background under the peak comes from the direct production of $3\pi^0$. Figure 13 shows the Dalitz plot of the $\eta' \to \eta\pi^0\pi^0$ decays. The Dalitz plot is uniform as expected.

Another important reaction to study is $\gamma p \to \pi^0\pi^0 p$. This process is one of the dominant ones in the MAMI-C energy range and carries valuable information about dynamics of $\pi\pi$ and πN interaction. An example of the Dalitz plot for the reaction is shown on Fig.12. The structure of the Dalitz plot is significantly different from the similar distribution obtained in $\pi^- p \to \pi^0\pi^0 n$ [7]. Finally Fig. 14 shows the first attempt to calculate the total cross section of the $\gamma p \to \pi^0 p$ reaction for the photon beam energies from 600 MeV to 1500 MeV. The Crystal Ball results are compared to the data obtained

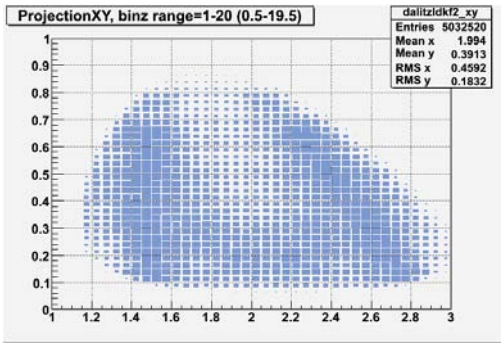

Figure 12: Dalitz plot distribution for the reaction $\gamma p \to \pi^0\pi^0 p$. Each event has two entries. The structure of the Dalitz plot is significantly different from the similar distribution in $\pi^- p \to \pi^0\pi^0 n$ [7].

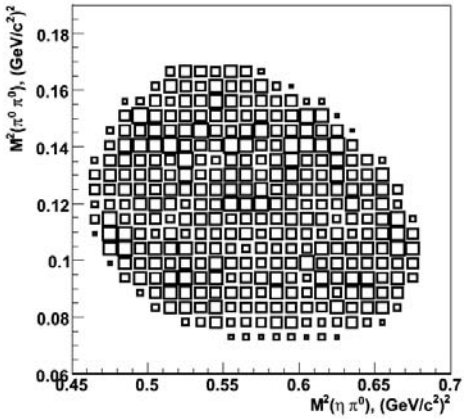

Figure 13: Dalitz plot distribution for the decay $\eta' \to \eta\pi^0\pi^0$. The total number of events is about 1100. Each event has two entries because of the two identical π^0. The sample represent about 20% of the available statistics.

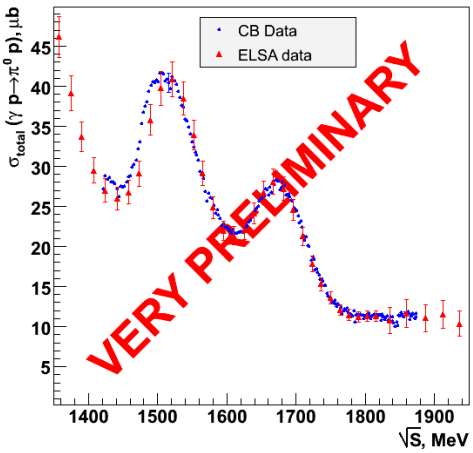

Figure 14: Preliminary results for the total cross section of $\gamma p \to \pi^0 p$ in the MAMI-C beam energy range obtained during the first round of the experiment. The Crystal Ball cross sections is normalized to the ELSA data at $\sqrt{s} = 1.5$ GeV.

with the Crystal Barrel/TAPS setup at ELSA. The Crystal Ball data are normalized to the ELSA results at $\sqrt{s} = 1.5$ GeV. The Crystal Ball results show superior quality of the data in statistical accuracy and the beam energy resolution. The high beam intensity and good energy resolution of the tagger allows a detailed investigation of the total cross section with the energy step of about 4 MeV. The energy resolution could be further improved by using the tagger microscope.

4 Summary

In summary, the Crystal Ball detector is a universal instrument, which makes possible precise measurements of multi–photon neutral states. The detector was successfully used with pion and kaon beams and in this paper we present the new high statistics, low–systematics measurement of the three kaon induced reactions: $K^- p \to \pi^0\Sigma$, $K^- p \to \pi^0\Lambda$, and $K^- p \to \overline{K}^0 n$. Besides the differential and total cross section we have measurement the polarization of the recoil hyperon for the reactions $K^- p \to \pi^0\Sigma$ and $K^- p \to \pi^0\Lambda$. While of superior quality, the new data shows reasonable agreement with existing measurements. A complete partial–wave analysis is needed to extract the parameters of the Λ^* ($\Lambda(1600)\frac{1}{2}^+$, $\Lambda(1670)\frac{1}{2}^-$, $\Lambda(1690)\frac{3}{2}^-$) and Σ^* ($\Sigma(1580)\frac{3}{2}^-$, $\Sigma(1620)\frac{1}{2}^-$, $\Sigma(1660)\frac{1}{2}^+$, $\Sigma(1670)\frac{3}{2}^-$) from the data.

The experiments with the Crystal Ball are continued at Mainz Microtron. In early 2007 we have started the new series of measurements with the upgraded MAMI-C machine which provides the high intensity high resolution beam of real photons with the maximum energy up to 1.5 GeV. The prelim-

inary MAMI-C results indicate early success of the program.

References

[1] G. Altarelli, Ann. Rev. Nucl. Part. Sci. **39** (1989) 357.

[2] D. J. Gross, Nucl. Phys. Proc. Suppl. **74** (1999) 426.

[3] B. M. K. Nefkens, "Concluding Comments" talk in this proceeding.

[4] T. Dombeck *et al.*, Phys. Rev. D **7** (1973) 1331.

[5] R. Armenteros *et al.*, Nucl. Phys. **B21** (1970) 15.

[6] S. Prakhov *et al.* Phys. Rev. C **72** (2005) 025201.

[7] S. Prakhov *et al.* Phys. Rev. C **69** (2004) 045202.

[8] A. Starostin *et al.* Phys. Rev. C **64** (2001) 55205.

[9] W. B. Tippens *et al.* Phys. Rev. Lett. **87** (2001) 193001.

[10] W-M Yoa *et al.*, J. Phys. G **33** (2006) 1.

[11] S. Prakhov, Crystal Ball report CB-05-002 at http://bmkn8.physics.ucla.edu/Crystalball/Docs/documentation.html.

[12] D. Alde *et al.*, Phys. Lett. **B 177** (1986) 115; D. Alde *et al.*, Z. Phys. C **36** (1987) 603.

[13] N. Cabibbo, Phys. Rev. Lett. **93** (2004) 121801.